SP2018_00102

ALTERNATIVE PROPELLANTS FOR GRIDDED ION ENGINES

Nazareno Fazio [(1)], Steve B. Gabriel [(1)], Igor O. Golosnoy [(1)]

[(1)] University of Southampton, University Road, SO17 1BJ, Southampton, UK,
Email:
n.fazio@soton.ac.uk
sbg2@soton.ac.uk
ig@ecs.soton.ac.uk

KEYWORDS: Electric propulsion, Gridded Ion Engine, Alternative Propellants, Xenon, Krypton

ABSTRACT:

Within the European GIESEPP project framework, a comparative overview of the properties of propellants suitable for electric propulsion and an assessment on the impact of substituting Xenon as operating medium will be presented in this paper.

A preliminary qualitative and quantitative analysis will be performed to assess the effects on the existing systems and to ensure their functionality with alternative propellants.

Based on a trade-off between performance and compatibility, Krypton was selected as main alternative and Iodine as secondary (due to possible compatibility problems). However, more extensive investigations will be required to address all the possible aspects of the propellant change.

1. INTRODUCTION

The development of the GIESEPP project, the first European Plug and Play Gridded Ion Engine (GIE) Standardised Electric Propulsion Platform, targets reducing the cost of GIE systems and increasing their production capacities. In the attempt to achieve these objectives, functionality of the GIESEPP systems with propellants alternative to Xenon is essential.

Xenon is the most common propellant used for space applications, particularly in GIE and Hall Effect Thruster (HET), thanks to its particular physical and chemical properties, such as low first ionization energy, high atomic mass, and chemical inertness. However, this gas is extraordinarily expensive due to its limited availability and highly expensive production process and this aspect can become a severe constriction when planning high-Δv missions, such as cargo missions and orbital transfer missions.

The objective of this paper is to assess the possibility of substituting Xenon as propellant through a preliminary investigation of the operations of the GIESEPP system and, in general, of a gridded ion thruster using different propellants. This analysis is to evaluate the impact on the existing systems and not to address what is required to design and develop an optimised system.

The paper is organised as follow. In Section 2, the selection process for choosing a suitable propellant is presented. Section 3 gives a qualitative summary of the impact of different propellants on the other parts of the electric propulsion system (EPS), such as the Flow Control Unit (FCU) and the Power Processing Unit (PPU), as well as a quick review of the compatibility and toxicity problems that each propellant could introduce. Section 4 is devoted to the analysis of the performance of gridded ion thrusters with the propellants selected in Section 2. Finally, general conclusion and possible perspectives are summarized in Section 5.

2. PROPELLANT SELECTION

The choice of the propellant in an electric propulsion (EP) system influences the performance of the thruster (e.g. specific impulse, thrust efficiency, power-to-thrust ratio) and, more in general, the complexity and cost of the entire system. Ideally, a propellant for ion engines should combine a low ionization threshold with a high ionization cross-section (to minimize the energy required to create a high-density plasma), a high molecular weight (to reduce the amount of propellant required), good handling and storage qualities (a liquid or solid propellant can offer higher density and, consequently, lower storage volume), high system and material compatibility, and a low spacecraft contamination potential. Keeping in mind that any propellant presents some drawbacks, Xenon has been used in the past few decades as it offers the best combinations of these properties, while its main disadvantages are its cost and its density (compared to liquid and solid propellants).

The selection of alternative propellants for this study has been based on the following criteria:

Table 1 – Selected propellants' physical properties [1] and cost [2]

Propellant (Z number)	Mass (amu)	State @ STP	1st / 2nd Ionization energies (eV)	Melting / boiling point (K)	Critical temperature (K) / pressure (MPa)	Density (g/cm^3) @ STP	Cost (per 100g)
Xe	131.3	Gas	12.13 / 20.97	161.4 / 165.1	289.7 / 5.8	0.0059	$120
Kr	83.8	Gas	14 / 24.36	115.8 / 119.7	209.5 / 5.5	0.0037	$33
Ar	39.9	Gas	15.76 / 27.63	83.8 / 87.3	150.7 / 4.9	0.0018	$0.5
Ne	20.2	Gas	21.56 / 40.96	24.6 / 27.1	44.5 / 2.7	0.0009	$33
He	4.0	Gas	24.59 / 54.41	0.95 / 4.2	5.2 / 0.2	0.0002	$5.2
H_2	2.0	Gas	15.43 / -	14 / 20.3	32.9 / 1.3	0.00009	$12
I_2 (I)	253.8 (126.9)	Solid	9.3 / - (10.45 / 19.13)	386.9 / 457.6	819 / 11.7	4.933	$8.3
C_{60}	720.6	Solid	7.5 / 12	sublimate @ 823	-	1.65	$1125
$C_{10}H_{16}$	136.2	Solid	9.23 / -	subl. @ 543.18	-	1.07	$100
Hg	200.6	Liquid	10.44 / 18.76	234.3 / 629.8	1764 / 167	13.534	$48

- Physical and chemical similarity to Xenon properties, i.e. noble gases plus Hydrogen;
- Heritage, i.e. Mercury, being used in the past (up to around 1980);
- Proximity to Xenon in the periodic table, i.e. Iodine;
- Others which have and are being investigated, i.e. Buckminsterfullerene and Adamantane.

In accord with these criteria, the analysis was carried out for the following selected propellants: Xenon (Xe), Krypton (Kr), Argon (Ar), Neon (Ne), Helium (He), Hydrogen (H_2), Iodine (I_2), Buckminsterfullerene (C_{60}), Adamantane ($C_{10}H_{16}$), Mercury (Hg). Their properties are reported in Table 1 (STP stands for Standard Temperature and Pressure, 273.15 K and 10^5 Pa).

3. IMPACT ON OTHER PARTS OF THE EPS

The analysis of the effects of substituting Xenon in an electric propulsion system starts with a qualitative assessment on the impact of using alternative propellants on the various elements of the system, such as performance, storage, FCU, PPU, cathode, plume (spacecraft interaction), lifetime, compatibility, handling and toxicity.

Performance

From a performance point of view, the other gaseous propellants are worse than Xenon for thrust efficiency, propellant utilization and thrust-to-power ratio, but better for specific impulse. Iodine and mercury have performance comparable to Xenon, while the exotic propellants are potentially superior to Xenon (except for specific impulse). The impact on the performance of the thruster is evaluated quantitatively in Section 4.

Storage

When considering the effect on the storage system, density has a predominant role: solid and liquid propellants have a clear advantage over gaseous ones, and, among the noble gases, Krypton is the element with the highest density after Xenon.

FCU

On the other hand, this reduced complexity of the tank associated to non-gaseous propellants can introduce specific requirements for the FCU and the transfer lines.

PPU

The impact on the PPU is low for solid and liquid propellants and it is mainly related to the additional power needed to vaporise them and to control the more complex FCU, while it can be relevant for the gaseous propellants due to the extra power required by the thruster (grid discharge, keepers voltage, etc.).

Cathode

When considering the effects on the cathode, the alternative propellants introduce important penalties: spot to plume transition, higher flow rates and higher heater power are linked to the gaseous alternatives, while problems of compatibility, contamination and, even, poisoning (in the case of Adamantane, being a hydrocarbon) are associated with solid and liquid propellants.

Plume (spacecraft interaction)

Condensable propellants can be problematic for thruster and spacecraft elements, such as solar arrays, optical instruments, radiators, etc., since

they can deposit if the surface temperature is below their melting point. The formation of this coating can have negative effects on the electrical and optical properties of these elements. In comparison, gaseous propellants should behave similarly to Xenon.

Lifetime

Similarly, the impact of the other gases on the lifetime of the system should be minimal, while Iodine can raise long term issue with thruster materials (especially with the cathode) and there are not enough data for the two exotic alternatives.

(Chemical) Compatibility

Noble gases do not present any issue because of their inertness, but Hydrogen's only concern is related to its high flammability. Comparatively, Fullerene, Adamantane and Mercury are not compatible with strong oxidizing agents, while Iodine is highly reactive and, as such, it is incompatible with a wide range of materials (metals, plastics, etc.).

Handling and toxicity

Being inert, the selected gases are not toxic, while the other propellants introduce different levels of toxicity: Adamantane is very toxic to environment and to aquatic life; Fullerene is categorised as a dangerous substance and it can cause serious eye and respiratory irritation, and, as such, specific attention is required when handling it; Iodine in large amount is poisonous, but in small doses is only slightly toxic, and the use of protective equipment is required when handling it; Mercury is a very toxic and accumulative poison (it is not easily eliminated by the body) and the use of specific equipment is mandatory.

In summary, based on this qualitative analysis, it can be concluded that, at least in terms of compatibility with the FCU, thruster materials and spacecraft, the alternative propellants with the least impact are the inert gases. However, from a performance point of view the best candidate is Iodine. If Iodine is to be dropped on the basis of incompatibility (handling and toxicity, potential spacecraft interactions, etc.), Krypton will be the selected one.

4. IMPACT ON PERFORMANCE

Propellant performance is traditionally measured by the thrust T, the specific impulse Isp, and power-to-thrust ratio.

As a reference for an immediate comparison, the operating point parameters of the QinetiQ's T5 and T6 thrusters will be used (Table 2). Both engines are Kaufman-type GIT: the T5 has 10 cm diameter grids, while the T6 has 22 cm diameter grids.

The following assumptions were made and their applicability is given in the following subsections:

Table 2 – Thrusters' operational data

Thruster	T5 [3]	T6 [4]
Nominal thrust T (mN)	25	145
Beam voltage V_b (V)	1100	1850
Beam current I_b (mA)	457	2158
Total propellant mass flow rate $\dot{m}_p$ (mg/s)	0.720	3.415
Thrust Correction Factor (TCF) γ	0.948*	0.945*
Thruster mass utilization efficiency η_m	0.864*	0.860*

* values calculated from experimental data [3, 4]

- Constant thruster geometry and operational points: this implies that the difference in performance between the various propellants is mainly a result of the difference in their atomic masses;
- Unmodified grid geometry (thicknesses, diameters, transparencies);
- Thrust correction factor γ and thruster mass utilization efficiency η_m kept fixed throughout the analysis and equal to the reference value obtained for Xenon and reported in Table 2 (exception made for Krypton's η_m in Section 4).

As a consequence of these assumptions, the analysis presented is general enough and could be applied to any propellant since it is essentially based only on the propellant's atomic mass and deals with the grid system, ignoring cathodes and the discharge chamber (except for Krypton as discussed in Section 4.4).

The results of this preliminary analysis are listed herein.

4.1. Beam Current

In order to calculate the performance of the various propellants, the perveance P, defined as the amount of current that an ion accelerator can extract and focus into a beam for a given applied voltage, and the ion current density j_i of a single beamlet were determined using the Child-Langmuir law [5]:

$$j_i = \frac{4}{9}\epsilon_0\sqrt{\frac{2e}{M}}\frac{V_T^{\frac{3}{2}}}{l_e^2} \qquad \text{Eq. 1}$$

where $P = \frac{I_b}{V_T^{\frac{3}{2}}} = \frac{4}{9}\epsilon_0\sqrt{\frac{2e}{M}}$, with e electron charge ($1.60\text{x}10^{-19}$ C), M ion mass, and ϵ_0 permittivity of free space ($8.8542\text{x}10^{-12}$ F/m), $V_T = V_{screen} + |V_{acc}|$ is the total voltage across the sheath between the screen grid and the acceleration grid, and

$l_e = \sqrt{\left(l_g + t_s\right)^2 + \frac{d_s^2}{4}}$ is the sheath thickness, l_g the grid gap, t_s the screen grid thickness, d_s the screen grid aperture diameter (Figure 1).

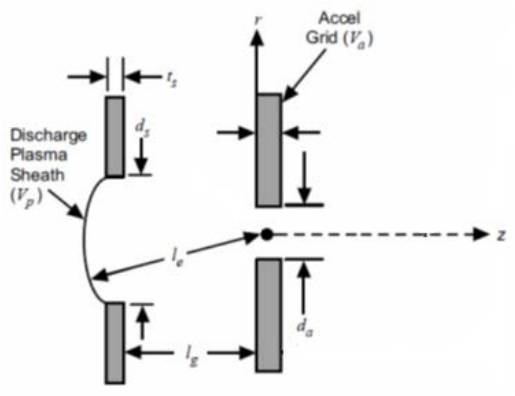

Figure 1 – Grid dimensions [5]

The grid dimensions and voltages for the two thrusters are reported in Table 4, while the computed values of perveance and ion current density for the different propellants are shown in Table 3 and Table 5, for the T5 and T6, respectively.

The next step was to calculate the beam current I_b, which can be written as:

$$I_b = j_i A_g T_s \qquad \text{Eq. 2}$$

where A_g is the grid area and T_s is the effective grid transparency (Table 4). T_s was derived using Eq. 2, with the values of the measured beam current (for Xenon) and of the grid area taken from the literature (given in Table 2 and Table 4, respectively). It was then assumed that T_s is constant for the different propellants and, hence, using the maximum perveance per hole given by j_i (Eq. 1), I_b can calculated to obtain the thruster (or, more correctly, the grid) performance for the different propellants for the T5 and T6 thrusters as shown in Table 3 and Table 5, respectively.

Table 4 – Grids properties for T5 [6] and T6 [7]

Thruster	T5 ø10cm	T6 ø22cm
Screen grid voltage V_{screen} (V)	1060	1810
Acceleration grid voltage V_{acc} (V)	-225	-265
Grid gap l_g (mm)	0.75	1
Screen grid thickness t_s (mm)	0.25	0.25
Screen grid aperture diameter d_s (mm)	2.15	1.97
Sheath thickness l_e (mm)	1.47	1.59
Ratio $\frac{V_T^{\frac{3}{2}}}{l_e^2}$ ($V^{3/2}/mm^2$)	21316.7	37360
Grid area A_g (mm^2)	2500π	12100π
Effective grid transparency T_s	0.574	0.3195

Table 3 – T5 performance with different propellants

Propellant	Xe	Kr	Ar	Ne	He	H_2	I	C_{60}	$C_{10}H_{16}$	Hg
M_a (amu)	131.3	83.8	39.9	20.2	4.0	2.0	126.9	720.6	136.2	200.6
M (kg) ($x10^{-25}$)	2.18	1.39	0.66	0.34	0.07	0.03	2.11	11.97	2.26	3.33
P ($A/V^{3/2}$) ($x10^{-9}$)	4.76	5.95	8.62	12.13	27.24	38.38	4.84	2.03	4.67	3.85
j_i (mA/cm^2)	10.14	12.69	18.38	25.86	58.07	81.82	10.31	4.33	9.95	8.20
I_b (mA)	457	572	829	1166	2618	3689	465	195	449	370
v_i (m/s)	40209	50330	72895	102563	230290	324490	40889	17163	39473	32530
$\dot{m}_i$ (mg/s)	0.622	0.497	0.343	0.244	0.109	0.077	0.611	1.457	0.634	0.769
P_b (W)	503	629	912	1282	2880	4058	511	215	494	407
T_{corr} (mN)	23.71	23.71	23.71	23.71	23.71	23.71	23.71	23.71	23.71	23.71
$\dot{m}_p$ (mg/s)	0.720	0.575 (0.606*)	0.397	0.282	0.126	0.089	0.708	1.687	0.733	0.890
Isp (s)	3359	4205 (3991*)	6090	8569	19241	27111	3417	1434	3298	2718
P_{tot} (W)	658	758 (825*)	1067	1438	3035	4213	667	370	649	562
$\frac{P_{tot}}{T_{corr}}$ (W/mN)	27.8	33.1 (34.8*)	45.0	60.6	128.0	177.7	28.1	15.6	27.4	23.7

* these values for Krypton are based on the results obtained in Sections 4.4 and 4.5: $\eta_m = 0.82$ and $P_d = 195.3\ W$

Table 5 – T6 performance with different propellants

Propellant	Xe	Kr	Ar	Ne	He	H_2	I	C_{60}	$C_{10}H_{16}$	Hg
M_a (amu)	131.3	83.8	39.9	20.2	4.0	2.0	126.9	720.6	136.2	200.6
M (kg) (x10^{-25})	2.18	1.39	0.66	0.34	0.07	0.03	2.11	11.97	2.26	3.33
P (A/V$^{3/2}$) (x10^{-9})	4.76	5.95	8.62	12.13	27.24	38.38	4.84	2.03	4.67	3.85
j_i (mA/cm^2)	17.77	22.24	32.21	45.33	101.77	143.40	18.07	7.58	17.44	14.38
I_b (mA)	2158	2701	3913	5505	12361	17417	2195	921	2119	1746
v_i (m/s)	52145	65271	94534	133008	298652	420815	53039	22258	51190	42187
$\dot{m}_i$ (mg/s)	2.937	2.346	1.620	1.151	0.513	0.364	2.887	6.880	2.992	3.630
P_b (W)	3993	4998	7238	10184	22867	32221	4061	1704	3919	3230
T_{corr} (mN)	144.71	144.71	144.71	144.71	144.71	144.71	144.71	144.71	144.71	144.71
$\dot{m}_p$ (mg/s)	3.415	2.728	1.884	1.339	0.596	0.423	3.357	8.001	3.478	4.221
Isp (s)	4323	5411	7837	11026	24758	34885	4397	1845	4244	3497
P_{tot} (W)	4628	5633	7873	10819	23502	32856	4696	2339	4554	3865
$\frac{P_{tot}}{T_{corr}}$ (W/mN)	32.0	38.9	54.4	74.8	162.4	227.0	32.5	16.2	31.5	26.7

4.2. Thrust

In a gridded ion thruster, the acceleration of ions to high exhaust velocity is achieved using an electrical power source. Considering that ion velocity is much higher that any unionized propellant escaping the thruster, the ideal thrust can be described as [5]:

$$T_{ideal} = \dot{m}_i v_i \qquad \text{Eq. 3}$$

where $\dot{m}_i$ is the ion mass flow rate and v_i is the ion velocity. Using the conservation of energy, the ion velocity is given by:

$$v_i = \sqrt{\frac{2eV_b}{M}} \qquad \text{Eq. 4}$$

where V_b, beam voltage, is the net voltage through which the ion is accelerated (fixed at 1100 V for T5 and 1850 V for T6), e is the electron charge, and M is the ion mass (kg). The ion mass flow rate is correlated to the ion beam current I_b by:

$$\dot{m}_i = \frac{I_b M}{e} \qquad \text{Eq. 5}$$

Eq. 3 is valid for an ideal case of a unidirectional, singly ionized, monoenergetic beam of ions. In order to take into account the presence of multiply charged species and for the beam divergence, a thrust correction factor (TCF) γ is introduced. Therefore, the total corrected thrust is given by [5]:

$$T_{corr} = \gamma \dot{m}_i v_i = \gamma \sqrt{\frac{2M}{e}} I_b \sqrt{V_b} \qquad \text{Eq. 6}$$

The factor γ was set identical for all the propellants and equal to 0.948 and 0.945, which are the experimental values obtained for the T5 and T6 thrusters, respectively, using Xenon [3, 4]. The use of these values should not introduce relevant errors in this first order approximation.

It is important to notice that the resulting thrust values for different propellants are consistent with a key feature of ion thrusters, i.e. the thrust density is independent of propellant mass.

4.3. Specific Impulse

The specific impulse Isp represents the thrust efficiency of a thruster and is expressed as the ratio of the thrust to the rate of propellant consumption [5]:

$$Isp = \frac{T}{\dot{m}_p g} = \frac{\gamma \eta_m}{g} \sqrt{\frac{2eV_b}{M}} = 1.417x10^3 \gamma \eta_m \sqrt{\frac{V_b}{M_a}} \qquad \text{Eq. 7}$$

where M_a is the ion mass (amu), g is the acceleration of gravity (9.807 m/s^2), and $\eta_m = \frac{\dot{m}_i}{\dot{m}_p}$ is the thruster mass utilization efficiency, which accounts for the ionized versus unionized propellant. Eq. 6 was used to obtain the final form. As before, the experimental value of η_m obtained for Xenon were used ($\eta_m = 0.864$ for T5 and $\eta_m = 0.86$ for T6). In the case of the thruster mass utilization efficiency, the assumption made is much stronger because it does not take into account how efficiently the thruster ionizes different propellants, but, again, this was made in order to obtain a first rough approximation and the order of magnitude of the specific impulse. For example, it can be

anticipated that discharge loss for the other gases will be higher than those typically obtained for Xenon [8].

4.4. Discharge Loss

In order to understand and quantify the impact of using a different propellant on thruster performance, it is desirable to have a model that describes the discharge chamber performance. In an ion thruster, this value is usually measured in terms of the power (in watts) necessary to produce, but not accelerate, an ion beam current of 1 A at a given propellant utilization efficiency. This power is defined by an ion production term $\eta_d = \frac{P_d}{I_b}$, called the discharge loss or the specific discharge power, that has units of watts per ampere (W/A) or electron-volts per ion (eV/ion). Since this term represents a power loss, it is desirable to minimize it while maintaining high propellant utilization. The plot of discharge loss versus the propellant utilization efficiency, known as the performance curve, usually characterises the discharge chamber performance of an ion thruster.

Different models for the discharge chamber performance have been developed in the past [5, 9]. Brophy's model [9] was the first comprehensive discharge chamber model based on particle and energy balance in the chamber. A uniform plasma and volume-averaged ionization and excitation rates were used in this model and, therefore, has been called a "0-D model". This model was initially developed for ring-cusp magnetic confinement, electron bombardment thrusters, but it can be applied to Kaufman-type thrusters as well with appropriate precautions and modifications.

According to this model, the discharge loss can be written as:

$$\eta_d = \frac{\epsilon_P^*}{f_B\{1-exp[-C_0\dot{m}(1-\eta_m)]\}} + \frac{f_C}{f_B}V_d \qquad \text{Eq. 8}$$

where

$$C_0 = \frac{4\sigma_0 l_c}{e v_0 A_g \phi_0} \qquad \text{Eq. 9}$$

and

$$\epsilon_P^* = \frac{\epsilon_0^* + \epsilon_M}{1-[\frac{V_C+\epsilon_M}{V_d}]}. \qquad \text{Eq. 10}$$

The quantity C_0, called the primary electron utilization factor, describes the interaction between primary electrons and neutral atoms and it depends on the primary electron containment length (l_c), the propellant gas (through σ_0, the total inelastic collision cross section for primary electron-neutral atom collisions [5, 10], and v_0, the neutral atom velocity), and the quality of the containment of neutrals (through A_g, grid area, ϕ_0, grid transparency to neutral atoms, and v_0).

The quantity ϵ_P^*, called the baseline ion energy cost, is related to different energy loss mechanisms such as: the energy cost expended in excitation compared to ionization of neutral atoms through ϵ_0^*, the average energy of Maxwellian electrons leaving the plasma at the anode ϵ_M, the cathode efficiency V_c that represents an additional potential drop from the hollow cathode insert to where the electrons enter the discharge chamber (e.g. for thrusters with a baffle assembly, V_c is the potential difference between the cathode exit and the exit of the baffle annulus region, through which the electrons are accelerated).

The other parameters present in Eq. 8 are: $f_B = \frac{I_b}{I_P}$ the extracted-ion fraction, and $f_C = \frac{I_c}{I_P}$ the fraction of ion current produces that goes to cathode potential surfaces, where $I_P = en_0 n_e \langle \sigma_+ v_e \rangle V_P$ is the ion production current, where n_0 and n_e are neutral density and plasma density, respectively, $\langle \sigma_+ v_e \rangle$ represents the product of the ionization collision cross section and the electron velocity averaged over the electron speed distribution, and V_P is the plasma volume.

In order to compare the performance of the discharge chamber with different propellants, a computer code based on Brophy's model has been used [11] with appropriate corrections and adaptations. The performance curves for T5 thruster using Xenon and Krypton are shown in Figure 2.

Since l_c, f_B and f_C cannot be predicted using this model, experimental values are required, but such data are not available for the T5 thruster. Their values were assumed to be 2.4 m, 0.5 and 0.1, respectively, which represent a reasonable assumption based on data present in literature [12]. Using these values, the model gives an output for η_d of 289 W/A at $\eta_m = 0.87$ for Xenon that is in good agreement with the one present in literature (286 W/A at $\eta_m = 0.864$, [3]).

These results were obtained keeping constant the parameters dependent on the thruster design and operational points, such as thruster geometry (A_g ϕ_0, and l_c), V_d, V_C, f_B, f_C, and varying those dependent on the propellant, such as $\dot{m}$, σ_0 and v_0 (in [12], it is demonstrated that these assumptions are acceptable for testing different propellants while keeping the same thruster). In particular, l_c can be kept constant for the two propellants because it depends on the magnetic field topology (mainly because the magnetic field affects primarily the electrons and not the ions) that, in our analysis, was assumed unchanged for the different propellants. These performance curves are qualitatively and quantitatively in good agreement with those present in the literature [12, 13], keeping in mind the variations due to different thrusters and operational points.

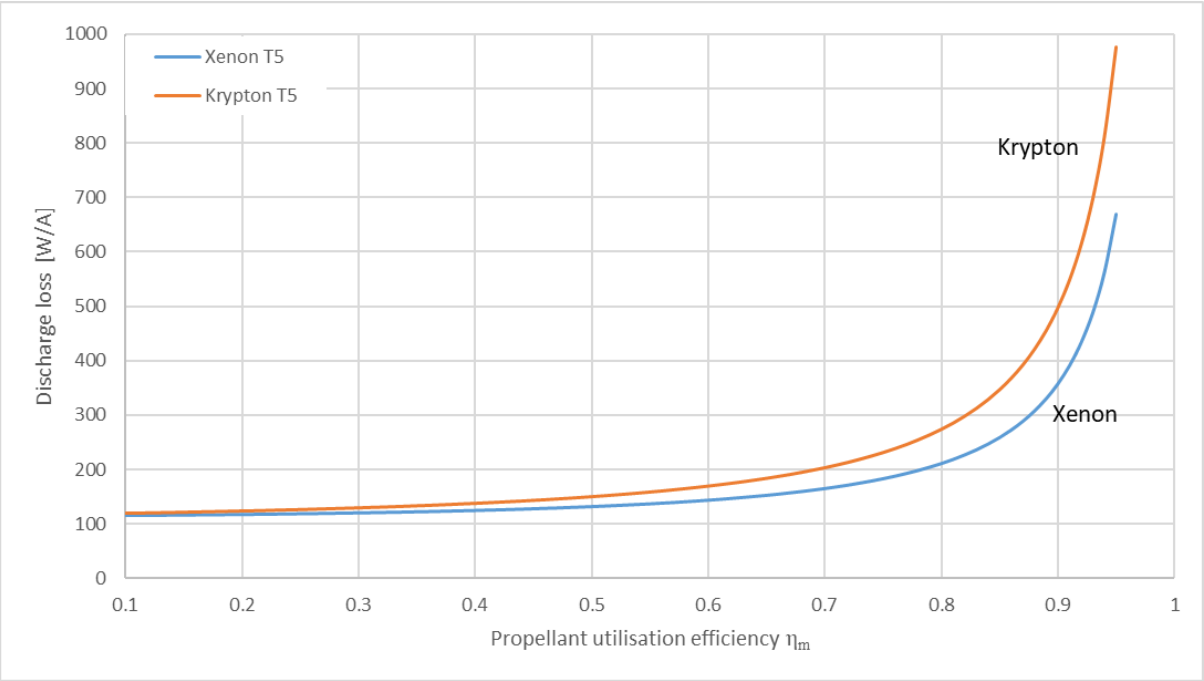

Figure 2 – Discharge loss as function of propellant utilization efficiency for T5 thruster

Thrusters are usually run near the "knee" of this curve in order to achieve high propellant utilization efficiency without excessive discharge loss. In fact, low discharge loss increases the electrical efficiency of the thruster and high mass utilization increases its fuel efficiency. In the case of the T5 thruster operated with the input described above, the "knee" is located around $\eta_m = 0.87$ when Xenon is used and it would be around $\eta_m = 0.82$ when Krypton is used, as shown in Figure 2. At the respective "knee", the discharge loss is 289 W/A for Xenon and 298 W/A for Krypton.

4.5. Total Power

The same assumptions described at the beginning of Section 4 were used in the calculation of total power and power-to-thrust ratio. The total power is obtained as:

$$P_{tot} = P_b + P_{other} \qquad \text{Eq. 11}$$

where $P_b = I_b V_b$ is the beam power calculated for the various propellants and P_{other} represents the other power input to the thruster required to create the thrust beam (e.g. electrical cost of producing the ions P_d, cathode heater and keeper power, grid power, etc.). As before, the used values for P_{other} are those of the engines running with Xenon, corresponding to 155.3 W for T5 and 645 W for T6 [3, 4]. The gathered results can be considered as guidance values (probably lower limits) in order to evaluate the impact of different propellants on engine performance.

In Figure 3 and Figure 4, specific impulse and beam power for the two thrusters are plotted as function of the atomic mass of a generic propellant.

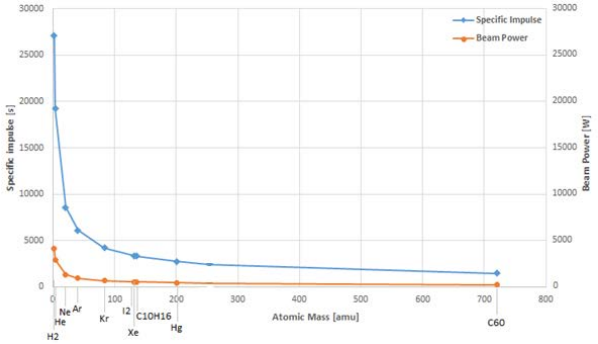

Figure 3 – Specific Impulse and Beam Power as function of the Atomic Mass for T5

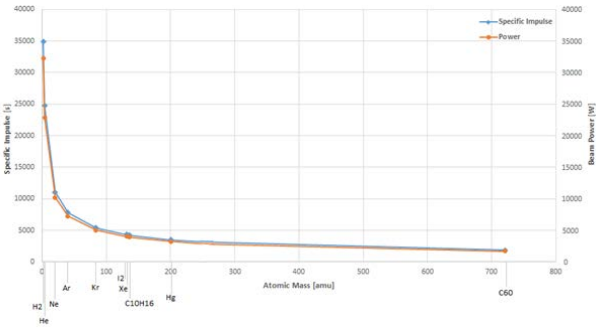

Figure 4 – Specific Impulse and Beam Power as function of the Atomic Mass for T6

In case of the T5 thruster, a better estimation of the total power required when using Krypton can be given based on the results obtained in Section 4.4: as a consequence of the higher discharge loss value for Krypton with respect to Xenon, the discharge power supply will need to deliver 170 W for a thruster running with Krypton compared to 130 W for Xenon and, assuming the same discharge potential of 43.5 V, a discharge current of 3.91 A for

Krypton will be required instead of 3 A for Xenon. Consequently, P_{other} will increase from 155.3 W for Xenon to 195.3 W for Krypton (assuming the same power needed to run cathode and neutralizer). Finally, this increment of P_{other} for Krypton combined with the higher value of the beam power calculated previously (Table 3, $P_{b_{Xenon}} = 503\,W$, $P_{b_{Krypton}} = 629\,W$) implies that the total power required to run the T5 thruster with Krypton will be 825 W compared to 658 W required with Xenon.

5. CONCLUSIONS

The impacts on the different parts of a GIE EPS have been investigated for a range of candidate propellants. A qualitative survey which looked at the physical properties, performance, storage, impacts on FCU and PPU, cathode operation, plume (spacecraft interaction), toxicity, and lifetime was followed by a more in-depth and quantitative analysis which calculated the effects on performance. Performance calculations were made using the QinetiQ's T5 and T6 thrusters as the base and by making certain assumptions, the key ones being that the grid geometry and potentials were the same as well as thruster efficiencies (thruster mass utilization efficiency η_m, and discharge loss η_d).

Based on these preliminary results, the only viable alternative would appear to be Krypton if all of the selected impacts are taken into consideration; however, Iodine and Mercury have the best performance but could be eliminated because of compatibility issues, especially in terms of spacecraft contamination and toxicity. Nevertheless, it should be noted that the former is current being actively pursued both in Europe and the USA as an alternative propellant despite these issues and that the latter was in the past (up to around 1980) the preferred propellant choice, only being replaced by Xenon due to spacecraft interactions. Additionally, the low storage density of Krypton has important effects on the storage system, i.e. need for a bigger and/or heavier propellant tank system.

Further investigation will be required to address in detail the impact of using alternative propellants with a particular focus on cathode-related problems and on refined models for the discharge chamber and grid system.

ACKNOWLEDGMENTS

The authors would like to thank the University of Southampton for the support. This research has been funded by the European Commission in the scope of the GIESEPP project, within the frame of the H2020 Research program - COMPET-3-2016-a SRC - In-Space Electrical Propulsion and Station Keeping, Incremental Line - Gridded Ion Engines of the European Union (Research and Innovation contract No 730002).

REFERENCES

1. Rumble, J.R. and J. Rumble, *CRC Handbook of Chemistry and Physics, 98th Edition*. 2017: CRC Press LLC.
2. Chemicool. *Chemicool Periodic Table*. 2017; Available from: www.chemicool.com.
3. Crofton, M.W., *Evaluation of the T5 (UK-10) Ion Thruster: Summary of Principal Results.* IEPC Paper, 1995: p. 95-91.
4. Lewis, R., J.P. Luna, and F. Guarducci. *Qualification of the T6 Thruster for BepiColombo*. in *34th International Electric Propulsion Conference and 6th Nano-satellite Symposium, Hyogo-Kobe, Japan*. 2015.
5. Goebel, D.M. and I. Katz, *Fundamentals of electric propulsion: ion and Hall thrusters*. Vol. 1. 2008: John Wiley & Sons.
6. Boyd, I. and M. Crofton, *Grid erosion analysis of the T5 ion thruster*, in *37th Joint Propulsion Conference and Exhibit*. 2001, American Institute of Aeronautics and Astronautics.
7. Coletti, M. *Simulation of the QinetiQ T6 Engine Ion Optics and Comparison to the Experimental Data [IEPC-2015-220]*. in *Proc. 30th International Symposium on Spece Technology and Science/2015 IEPC, Kobe/Japan*. 2015.
8. Owens, J.W., *A noble gas ion propulsion system*, in *10th Electric Propulsion Conference*. 1973.
9. Brophy, J.R. and P.J. Wilbur, *Simple performance model for ring and line cusp ion thrusters.* AIAA Journal, 1985. **23**(11): p. 1731-1736.
10. Biagi, S.F. *Cross sections extracted from PROGRAM MAGBOLTZ, VERSION 7.1 JUNE 2004*. 2018; Available from: www.lxcat.net/Biagi-v7.1.
11. Sánchez Lara, C., *Design and performance analysis study of an ion thruster*. 2016, Universitat Politècnica de Catalunya.
12. Brophy, J.R., *Ion thruster performance model*. 1984.
13. Sovey, J.S., *Improved ion containment using a ring-cusp ion thruster.* Journal of Spacecraft and Rockets, 1984. **21**(5): p. 488-495.